

Pressure-temperature magnetostructural phase diagrams of slowly cooled $\text{Co}_{1-x}\text{Cu}_x\text{MnGe}$ ($0.05 \leq x \leq 0.35$)

Ryszard Duraj,¹ Aleksandra Deptuch,² Andrzej Szytuła,³ Bogusław Penc,³ and Stanisław Baran^{3,*}

¹*Institute of Physics, Cracow University of Technology, Podchorążych 1, PL-30-084 Kraków, Poland*

²*Institute of Nuclear Physics Polish Academy of Sciences, Radzikowskiego 152, PL-31-342 Kraków, Poland*

³*M. Smoluchowski Institute of Physics, Jagiellonian University, prof. Stanisława Łojasiewicza 11, PL-30-348 Kraków, Poland*

(Dated: July 12, 2022)

Polycrystalline samples of $\text{Co}_{1-x}\text{Cu}_x\text{MnGe}$ ($x = 0.05, 0.10, 0.15, 0.22$ and 0.35), prepared by arc melting under argon atmosphere, have been annealed at 1123 K with final furnace cooling. The samples have been investigated by powder X-ray diffraction (in function of temperature) and ac magnetic measurements (in function of temperature and applied hydrostatic pressure up to 12 kbar). On the basis of the experimental data, the (p, T) phase diagrams have been determined. For the low Cu content ($x = 0.05, 0.10$ and 0.15), the compounds show a martensitic transition between the low-temperature orthorhombic crystal structure of the TiNiSi -type (space group: $Pnma$) and the high-temperature hexagonal structure of the Ni_2In -type (space group: $P6_3/mmc$). For the high Cu content ($x = 0.22$ and 0.35) only the hexagonal structure is observed. All compounds undergo a transition from para- to ferromagnetic state with decreasing temperature (in case of $x = 0.22$ through an intermediate antiferromagnetic phase). The para- to ferromagnetic transition is fully coupled with the martensitic one for $x = 0.05$ at the intermediate pressure range ($6 \text{ kbar} \leq p \leq 8 \text{ kbar}$). Partial magnetostructural coupling is observed for $x = 0.10$ at ambient pressure. The Curie temperature at ambient pressure decreases from 313 K for $x = 0.05$ (in the orthorhombic phase) to about 250 K for the remaining compounds (in the hexagonal phase). For the $\text{Co}_{0.85}\text{Cu}_{0.15}\text{MnGe}$ compound, entropy change associated with the martensitic transition has been calculated using Clausius-Clapeyron equation.

keywords: intermetallic compounds, X-ray diffraction (XRD), magnetic materials, magnetic properties, pressure-temperature phase diagram

I. INTRODUCTION

The magnetostructural transformation materials, i.e. the materials that undergo the crystallographic and magnetic phase transitions simultaneously, are of considerable attention not only for their importance in fundamental physics, but also for their applications as multifunctional materials. Magnetostructural transformation, originating from coupling between spins and lattice, is found in a number of ternary $\text{MM}'\text{Ge}$ compounds, where M and M' are 3d transition elements. CoMnGe and its derivative compounds form a family of compounds whose magnetostructural properties can be easily tuned by changing composition, thermodynamic parameters, sample preparation procedure, etc. The CoMnGe parent compound crystallizes in two crystal structures: an orthorhombic one of the TiNiSi -type (space group: $Pnma$, No. 62) and a hexagonal one of the Ni_2In -type (space group: $P6_3/mmc$, No. 194), below and above the martensitic phase transition temperature (T_s) above 400 K, respectively (the exact transition temperature depends on sample preparation procedure) [1]. The compound in both crystal variants is ferromagnetic with the Curie temperatures (T_C) of 337 and 283 K and magnetic moments per molecule equal to $3.71(2)$ and $2.80(5) \mu_B$

for the orthorhombic and hexagonal phases, respectively (see Table 2 in [2]). Neutron diffraction data indicate existence of a ferromagnetic order with the magnetic moment in the Mn sublattice present in both phases, while the Co atoms possess magnetic moments only in the orthorhombic phase [3, 4]. CoMnGe is located in vicinity of a critical point in the magnetostructural phase diagram for pseudoternary germanides $\text{M}_{1-x}\text{M}'_x\text{MnGe}$ (see Fig. 1 in Ref. [5]). In the stoichiometric CoMnGe compound a magnetostructural coupling at ambient pressure is absent as T_s and T_C are well separated. The magnetostructural transition can be induced by application of external pressure exceeding 6 kbar [6]. Alternatively, the magnetostructural coupling can be achieved by doping of substitutional and/or interstitial atoms as well as introducing metal vacancies [7]. Investigation of magnetic properties of CoMnGe and its derivatives is of great importance due to large magnetocaloric effect around room temperature [8–10].

Recently, it has been reported that doping Cu atoms into the Co sublattice in $\text{Co}_{1-x}\text{Cu}_x\text{MnGe}$ ($0 \leq x \leq 0.5$) leads to complex magnetic behavior including appearance of new magnetic phases and magnetostructural coupling [11, 12]. These intriguing properties have inspired us to undertake the current study in which we report investigation of physical properties of $\text{Co}_{1-x}\text{Cu}_x\text{MnGe}$ ($0.05 \leq x \leq 0.35$) by X-ray diffraction and ac magnetic susceptibility measurements under hydrostatic pressure.

* stanislaw.baran@uj.edu.pl

On the basis of these data, the magnetostructural phase diagrams (p, T) are determined. This work is a continuation of our broader scientific project concentrated on the role of external pressure on physical properties of the pseudoternary $M_{1-x}M'_x\text{MnGe}$ systems [13, 14].

II. EXPERIMENTAL DETAILS AND RESULTS

A. Crystal structure

Polycrystalline samples of $\text{Co}_{1-x}\text{Cu}_x\text{MnGe}$ ($x = 0.05, 0.10, 0.15, 0.22$ and 0.35) have been prepared by arc melting of constituent elements (purity better than 99.9 wt %) under argon atmosphere, followed by annealing in high vacuum ($\sim 10^{-3}$ mbar) for 5 days at 1123 K (850 °C) and subsequent furnace cooling down to room temperature. Sample quality has been tested at room temperature by powder X-ray diffraction (XRD) using X'Pert PRO (PANalytical) diffractometer ($\text{CuK}\alpha$ radiation).

In order to investigate temperature evolution of the XRD patterns of $\text{Co}_{1-x}\text{Cu}_x\text{MnGe}$ ($0.05 \leq x \leq 0.35$), the powder samples have been placed in capillaries mounted in Empyrean 2 (PANalytical) diffractometer ($\text{CuK}\alpha$ radiation, parallel incident beam, geometry of a horizontal rotating capillary, $2\theta = 15\text{--}95^\circ$ or $28\text{--}90^\circ$). Temperature has been controlled with the Cryostream 700 Plus (Oxford Cryosystems) attachment with 5 min. of stabilization before collection of each pattern. The patterns have been collected on heating and subsequent cooling between 80 and 480 K.

Representative X-ray diffraction patterns (XRD) of $\text{Co}_{1-x}\text{Cu}_x\text{MnGe}$ ($x = 0.05, 0.10$ and 0.15) collected at selected temperatures are shown in Fig. 1. For all compounds a clear change of the crystal structure with increasing temperature is evident. In order to follow temperature evolution of the crystal structure, a Rietveld-type computer program FullProf [15] has been used to process the XRD data. Fig. 2 shows a sample XRD pattern together with the results of Rietveld refinement. The compounds investigated in this work crystallize in two types of the crystal structure:

- the low-temperature orthorhombic phase of the TiNiSi-type (space group $Pnma$) in which each element occupies the $4c$ site ($x, \frac{1}{4}, z$) with different values of the x and z parameters,
- the high-temperature hexagonal phase of the Ni_2In -type (space group $P6_3/mmc$) with the Co atoms occupying the $2d$ site ($\frac{1}{3}, \frac{2}{3}, \frac{3}{4}$), the Mn atoms at the $2a$ site (0, 0, 0) and the Ge atoms at the $2c$ site ($\frac{1}{3}, \frac{2}{3}, \frac{1}{4}$).

Rietveld refinement of the XRD patterns has allowed to determine temperature evolution of the structural parameters as well as the phase fraction (see Fig. 3 and Tables I, II and III). The TiNiSi-type crystal structure,

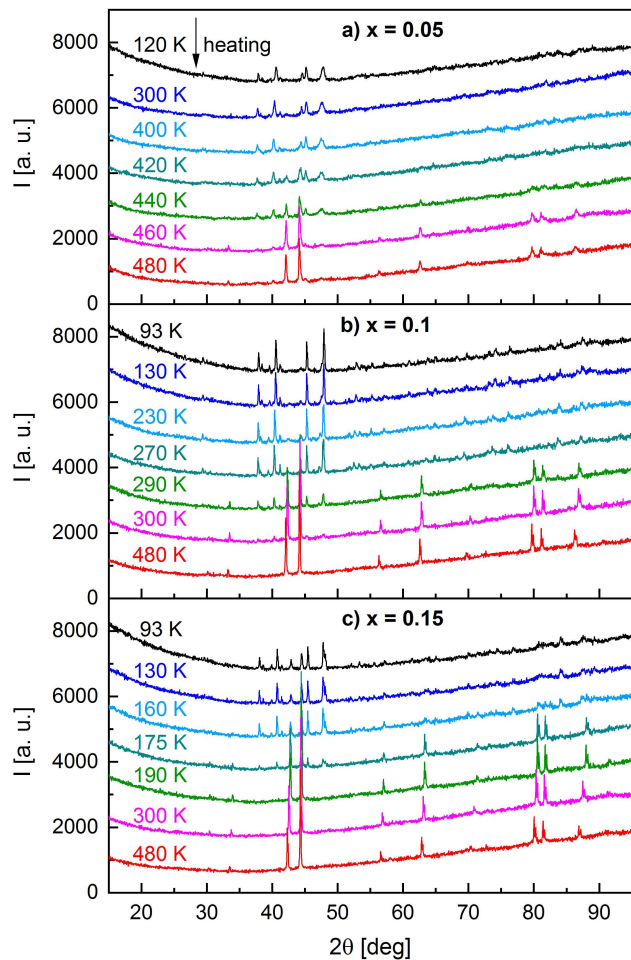


FIG. 1. Representative powder XRD patterns of $\text{Co}_{1-x}\text{Cu}_x\text{MnGe}$ ($x = 0.05\text{--}0.15$) collected on heating.

which is dominant at low temperatures, transforms into the hexagonal Ni_2In -type structure with increasing temperature. The transformation process is characterized by the presence of a distinct hysteresis (see the upper insets in Fig. 3), characteristic of the first-order phase transition. The critical temperature of the phase transition decreases with increasing Cu content.

Considering the relationship $a_o = c_h$, $b_o = a_h$, $c_o = \sqrt{3}a_h$ and $V_o = 2V_h$ (where the “o” and “h” indices refer to the orthorhombic and hexagonal structures, respectively), it is found that the martensitic transformation is accompanied by a large volume expansion $\frac{V_o - 2V_h}{V_o}$ of about 4 %, as well as strains of the lattice $\frac{a_o - a_h}{a_o}$ and $\frac{b_o - b_h}{b_o}$ equal to about 11 % and 7 %, respectively. Such results indicate large entropy change associated with the martensitic transformation. In case the magnetocaloric coupling is present, a large entropy magnetocaloric effect is expected to accompany the transformation.

Fig. 4 shows the XRD patterns of $\text{Co}_{1-x}\text{Cu}_x\text{MnGe}$ ($x = 0.22$ and 0.35) collected at 80 and 480 K, together

TABLE I. Lattice parameters a_o , b_o and c_o , unit cell volume V_o , weight fraction and agreement factors of Rietveld refinement obtained for the orthorhombic phase of $\text{Co}_{1-x}\text{Cu}_x\text{MnGe}$ from the X-ray diffraction data collected at the lowest investigated temperature and close to the martensitic transition for $x = 0.05$ -0.15 on heating.

x	T [K]	a_o [Å]	b_o [Å]	c_o [Å]	V_o [Å ³]	fraction [%]	R_{Bragg} [%]	R_f [%]
0.05	100	5.931(3)	3.823(2)	7.076(3)	160.4(2)	88.2(2.3)	8.7	6.8
	440	6.026(5)	3.842(3)	7.089(4)	164.1(2)	52.6(3.1)	18.3	15.6
0.1	83	5.9569(7)	3.8013(4)	7.0740(8)	160.18(3)	96.4(1.4)	9.4	8.6
	290	6.0204(9)	3.8139(4)	7.0708(9)	162.35(4)	33.0(1.3)	20.2	20.8
0.15	83	5.9069(9)	3.8091(4)	7.0363(8)	158.32(4)	82.2(2.0)	12.3	11.0
	175	5.919(2)	3.8130(5)	7.038(1)	158.85(5)	22.3(1.1)	36.0	34.7

TABLE II. Lattice parameters a_h and c_h , unit cell volume V_h , weight fraction and agreement factors of Rietveld refinement obtained for the hexagonal phase of $\text{Co}_{1-x}\text{Cu}_x\text{MnGe}$ from the X-ray diffraction data collected at 480 K for $x = 0.05$ -0.35 and close to the martensitic transition for $x = 0.05$ -0.15 on heating.

x	T [K]	a_h [Å]	c_h [Å]	V_h [Å ³]	fraction [%]	R_{Bragg} [%]	R_f [%]
0.05	440	4.103(2)	5.390(3)	78.59(7)	47.4(2.0)	6.9	8.5
	480	4.1065(9)	5.394(2)	78.78(4)	100	6.6	10.5
0.1	290	4.0962(2)	5.3569(3)	77.852(8)	67.0(1.6)	6.7	8.3
	480	4.1052(2)	5.3976(3)	78.778(8)	100	7.9	9.7
0.15	175	4.0802(2)	5.2855(2)	76.204(5)	77.7(1.8)	7.9	10.1
	480	4.0940(2)	5.3582(3)	77.777(8)	100	8.6	11.7
0.22	480	4.1115(2)	5.4070(3)	79.156(8)	100	7.1	11.7
0.35	480	4.107(2)	5.428(3)	79.28(7)	100	12.0	13.0

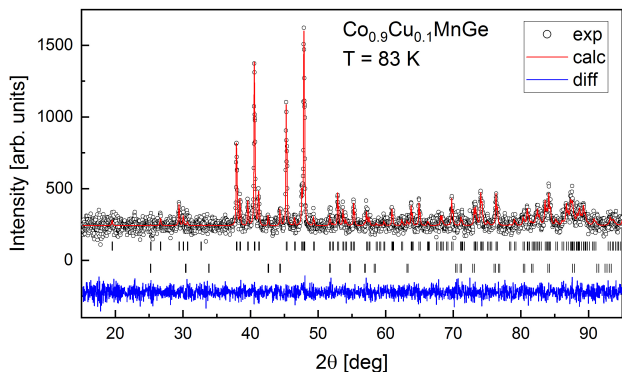


FIG. 2. XRD pattern of $\text{Co}_{0.9}\text{Cu}_{0.1}\text{MnGe}$ collected at 83 K together with the results of Rietveld refinement. For better clarity, the refined background has been subtracted from both the experimental and calculated patterns after the final refinement. The first and second rows of the vertical bars indicate the Bragg reflection positions originating from the low-temperature orthorhombic phase ($Pnma$, weight fraction 96.4(1.4)%) and the high-temperature hexagonal phase ($P6_3/mmc$, weight fraction 3.6(5)%), respectively.

with the Rietveld refined data of the pattern taken at 80 K. The experimental data indicate that the hexagonal crystal structure is stable in the whole temperature range. The lattice parameters a_h and c_h as well as unit cell volume V_h (see Fig. 5) show nearly linear thermal expansion.

B. Magnetic properties

High pressure measurements have been carried out in the temperature range 80–400 K in fully hydrostatic conditions. Helium has been used as a pressure-transmitting medium. The experimental cell has been connected to the UNIPRESS OCA GCA-10 three stage gas compressor by a manganin gauge placed in the highest pressure stage of the compressor. A thermocouple placed directly at the sample position has served as a temperature sensor. The ac magnetic susceptibility measurements have been carried out in a weak magnetic field (of 1 mT amplitude and frequency of 300 Hz). The voltage induced in the pick-up coils has been measured by a lock-in amplifier.

Figs. 6a–e show temperature dependence of the ac magnetic susceptibility collected on heating and cooling for the samples with $x = 0.05$, 0.10, 0.15, 0.22 and 0.35 at selected hydrostatic pressures up to 12 kbar. For all compounds a sharp increase of susceptibility is observed at the ambient pressure below 315 K ($x = 0.05$), 251 K (0.10), 260 K (0.15) and 250 K (0.35) (the transition temperatures have been defined as temperatures of the inflection points in the $\chi(T)$ curves; in case of $x = 0.22$, the transition has two-step character and is discussed in details later in this section). Such a behavior is characteristic of para- to ferromagnetic transition as observed in the hexagonal stoichiometric CoMnGe [4]. For the samples with $x \geq 0.10$ another anomalies appear with further decrease of temperature. A decrease of magnetic susceptibility with hysteresis of a few kelvins is found around 180 K for $x = 0.10$ indicating a development of antifer-

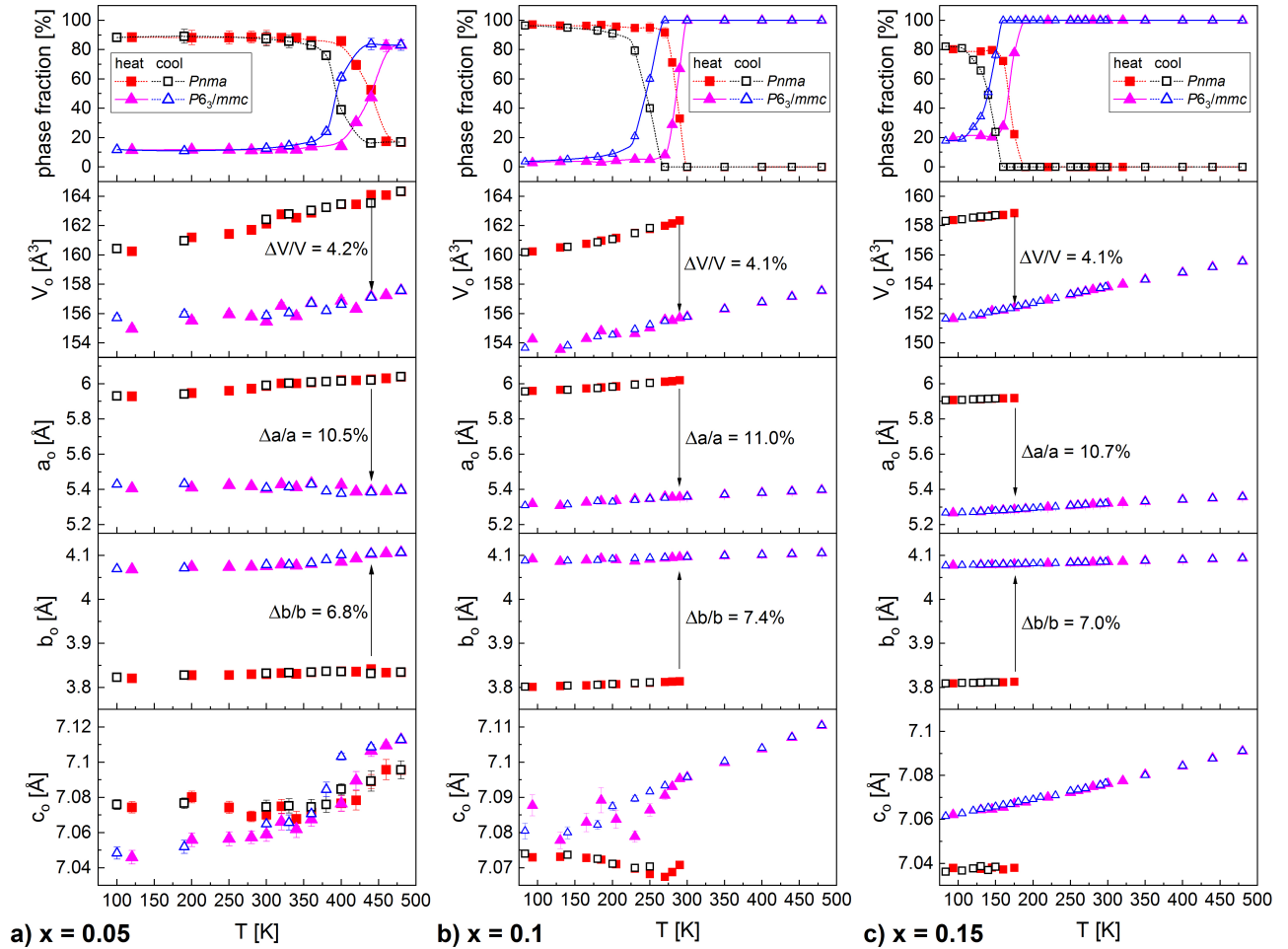


FIG. 3. Thermal evolution of the phase fraction (weight percentage), volume of the unit cell and lattice constants for $\text{Co}_{1-x}\text{Cu}_x\text{MnGe}$ ($x = 0.05\text{--}0.15$). Unit cell parameters of the hexagonal phase have been recalculated to those of the orthorhombic phase using the following relations: $a_o = c_h$, $b_o = a_h$, $c_o = \sqrt{3}a_h$ and $V_o = 2V_h$.

TABLE III. Parameters derived from Rietveld refinement of the XRD patterns: temperatures of the structural phase transition on heating $T_s^{(h)}$ and cooling $T_s^{(c)}$ together with phase fractions found at low temperatures (80-100 K) and 480 K.

x	0.05	0.10	0.15	0.22	0.35
temperature range [K]	100-480	83-480	83-480	80-480	80-480
$T_s^{(h)}$	440	286	167	-	-
$T_s^{(c)}$	393	245	140	-	-
weight fraction of hexagonal phase at 80-100 K [%]	11.8(8)	3.6(5)	17.8(7)	100*	100*
weight fraction of hexagonal phase at 480 K [%]	83.2(3.7)	100	100	100*	100*

*Small impurity peaks have been observed but they have been excluded from fitting, as they are too weak to be identified unambiguously.

romagnetic component of the magnetic structure at low temperatures. For $x = 0.15$ an increase of susceptibility with wide temperature hysteresis (~ 30 K) is observed. This anomaly well coincides with the structural martensitic transition detected from the XRD data (compare Figs. 3b and 6b). The magnetic data for $x = 0.22$ reveal

complex magnetic properties – with decrease of temperature a maximum at $T_1 = 248$ K is followed by an inflection point at $T_2 = 238$ K and another inflection point at much lower temperature $T_t = 132$ K. Such a behavior suggests the following sequence of magnetic ordering: para-antiferro-ferro- and finally ferrimagnetic phase. The

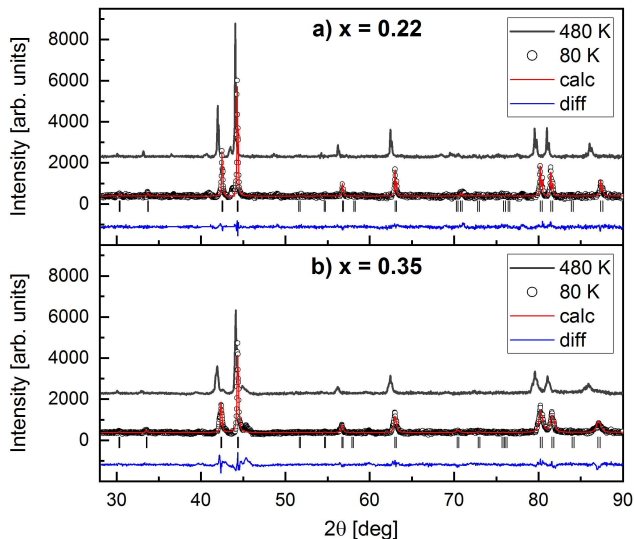


FIG. 4. XRD patterns of $\text{Co}_{1-x}\text{Cu}_x\text{MnGe}$ ($x=0.22$ and 0.35) collected at 480 and 80 K, together with the results of Rietveld refinement of the patterns taken at 80 K. For better clarity, the refined background has been subtracted from both the experimental and calculated patterns after the final refinement. The vertical bars indicate the Bragg reflection positions originating from the hexagonal phase (space group $P6_3/mmc$).

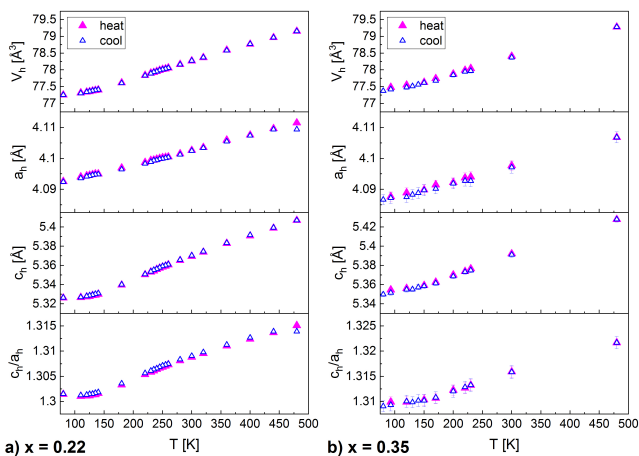


FIG. 5. Thermal evolution of the volume of the hexagonal unit cell, lattice constants and their ratio for $\text{Co}_{1-x}\text{Cu}_x\text{MnGe}$ ($x=0.22$ and 0.35).

sample with $x = 0.35$ undergoes a para-ferromagnetic transition at $T_C = 250$ K followed by the transition to the final ferrimagnetic state at $T_t = 159$ K.

Application of hydrostatic pressure has a significant influence on the magnetic properties, namely:

- $x = 0.05$: For low pressures (up to 4 kbar), the Curie temperatures derived from the $\chi(T)$ curves collected on cooling and heating agree within the

accuracy of measurement. No thermal hysteresis indicates a second-order phase transition. With increasing pressure ($p > 6$ kbar) a distinct thermal hysteresis (up to 20 K), characteristic of the first-order magnetostructural phase transition, develops. Moreover, for the highest pressures (10 and 12 kbar), the transition from the paramagnetic state undergoes in two stages: with decreasing temperature a typical second-order para-ferromagnetic transformation with no thermal hysteresis occurs in the hexagonal Ni_2In -type phase, while further decrease of temperature leads to appearance of the first-order magnetostructural phase transition associated with visible hysteresis (see Fig. 6a).

- $x = 0.10$: A para-ferromagnetic transition shows a small hysteresis (~ 4 K) at ambient pressure indicating partial magnetostructural coupling. With increasing pressure ($p = 1.5$ and 3 kbar) this transition turns into two-step transition, as observed previously for $x = 0.05$ at high pressures (10 and 12 kbar), revealing temperature separation of the purely magnetic and magnetostructural transitions. For $p \leq 3$ kbar additional transition to probably ferrimagnetic state appears at $T_t \approx 180$ K. A small hysteresis (~ 5 K) suggests a first-order character of the latter transition. For higher pressures ($6 \text{ kbar} \leq p \leq 9 \text{ kbar}$) a purely magnetic para-ferromagnetic transition (no temperature hysteresis visible) remains well-separated from the ferro-ferrimagnetic magnetostructural transition (hysteresis of 10 K (6 kbar) or 25 K (9 kbar)). For the highest pressure (12 kbar) only para-ferromagnetic transition is visible, while the magnetostructural transition seems to be below the temperature range experimentally available (see Fig. 6b).
- $x = 0.15$: A second order (no temperature hysteresis) para- to ferromagnetic transition undergoes at $T_C = 264$ K, while the first order magnetostructural transition with distinct temperature hysteresis is visible below 200 K. The temperature of the magnetostructural transition well coincides with martensitic transition detected from the XRD data (compare Figs. 3c and 6c).
- $x = 0.22$ and 0.35 : Application of external pressure influences transition temperatures, while the shape of the $\chi(T)$ curves remains unchanged (see Figs 6d and 6e). All observed magnetic transitions show no detectable temperature hysteresis. For $x = 0.22$, decrease of temperature reveals a maximum in $\chi(T)$ at $T_1 = 248$ K followed by a rapid increase of magnetic susceptibility at T_2 being about 10 K below T_1 . The first anomaly suggests para- to antiferromagnetic transition at T_1 with further transformation to ferro- or ferrimagnetic state at T_2 . Below 150 K another anomaly (inflection point) is visible at T_t . The observed de-

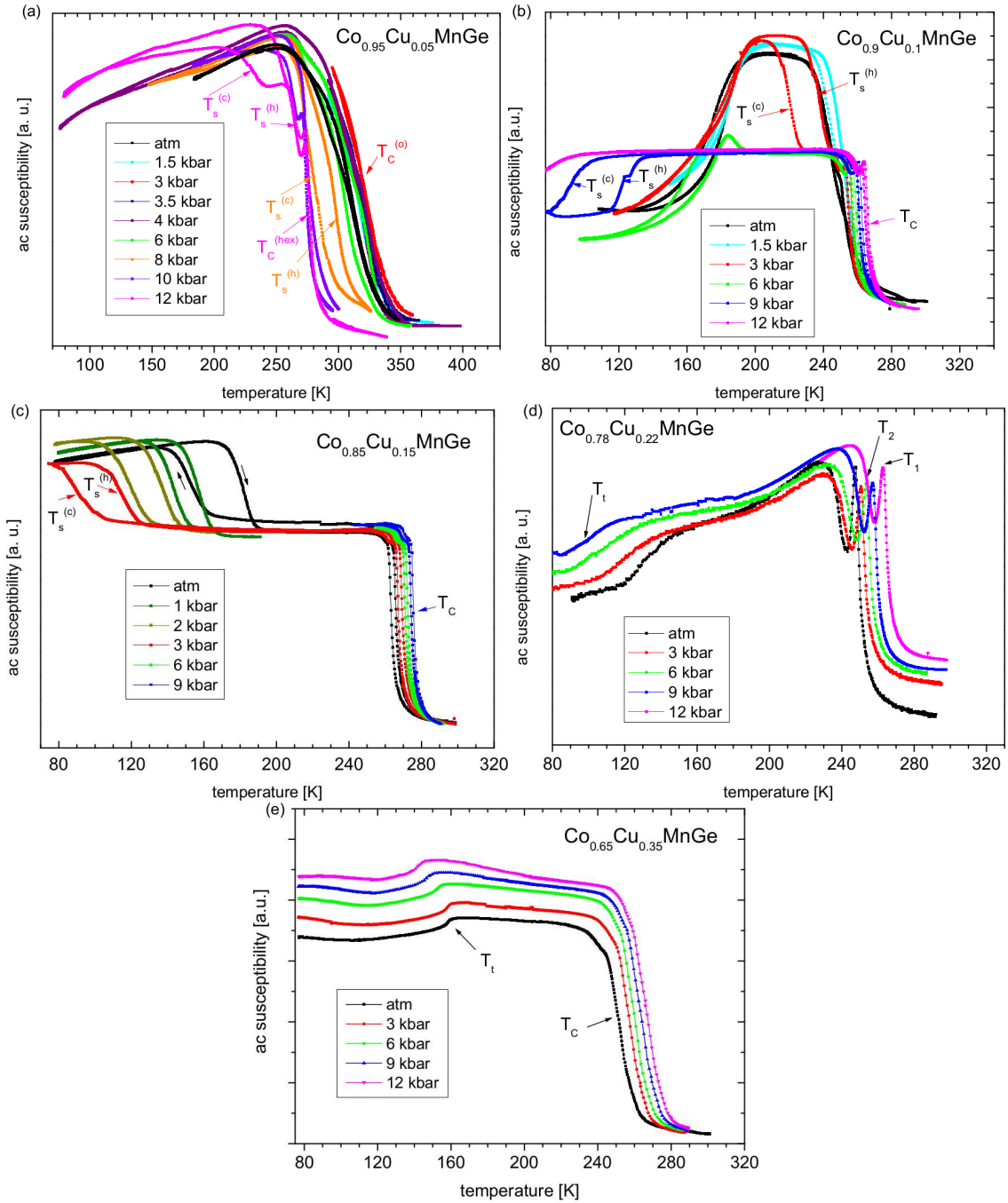


FIG. 6. Temperature dependence of the ac magnetic susceptibility of slowly cooled $\text{Co}_{1-x}\text{Cu}_x\text{MnGe}$ for (a) $x = 0.05$, (b) $x = 0.10$, (c) $x = 0.15$, (d) $x = 0.22$ and (e) $x = 0.35$ at selected hydrostatic pressures up to 12 kbar.

crease of susceptibility suggests development of antiferromagnetic contribution to the magnetic structure. For $x = 0.35$, a rapid increase of susceptibility at $T_C = 250$ K proves existence of para- to ferromagnetic transition, followed by a second transition (visible as inflection point in $\chi(T)$) at $T_t = 159$ K – the latter one evidencing for development of anti-ferromagnetic contribution to the magnetic struc-

ture. It is worth noting that all the above mentioned magnetic transitions refer to the hexagonal crystal structure which is found to exist within the investigated temperature interval at ambient pressure (according to the XRD data) and no signs of structural transition are detected under applied hydrostatic pressure.

On the basis of the experimental data, the magne-

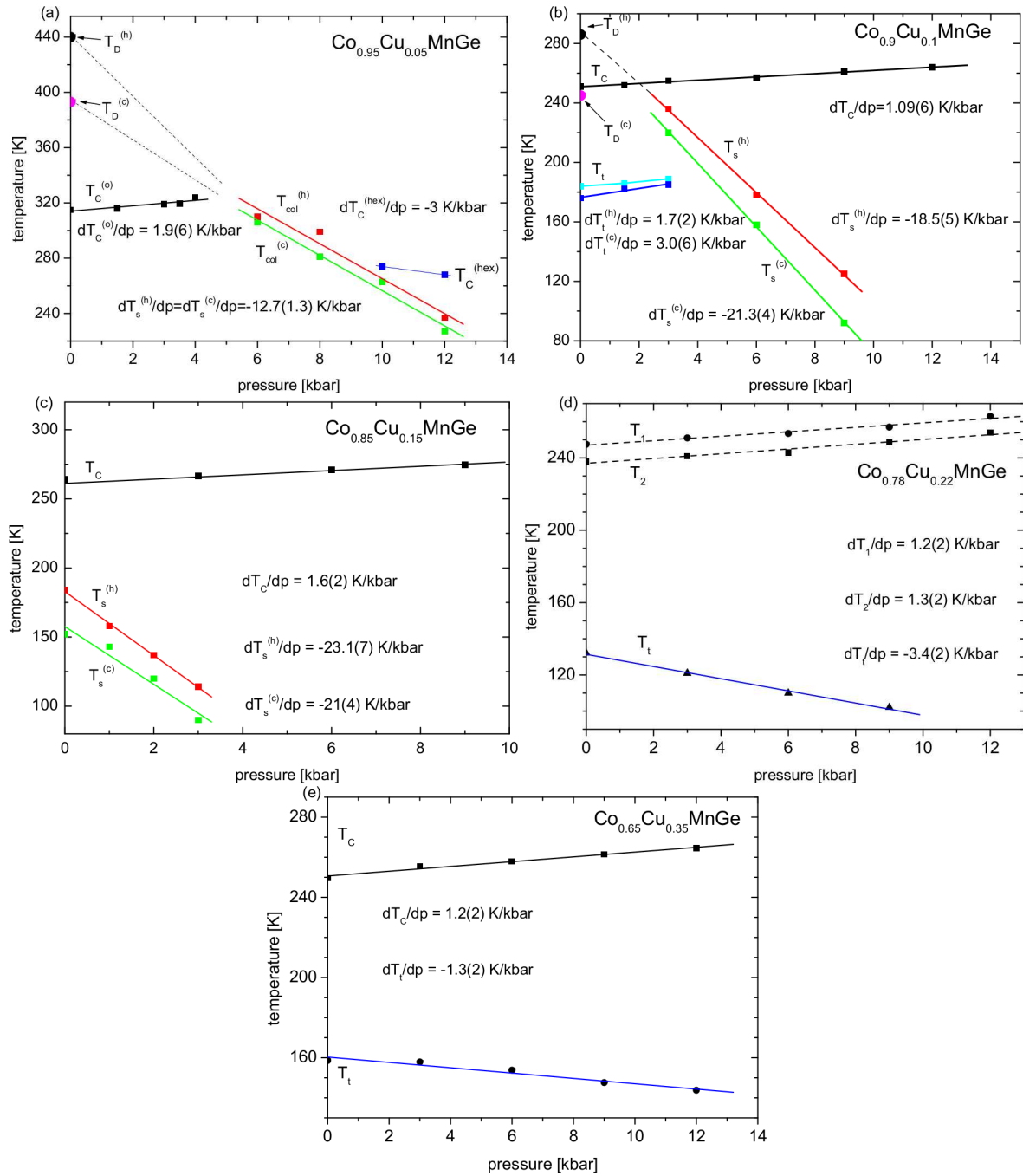


FIG. 7. Magnetostructural (p, T) phase diagrams of slowly cooled $\text{Co}_{1-x}\text{Cu}_x\text{MnGe}$ for (a) $x = 0.05$, (b) $x = 0.10$, (c) $x = 0.15$, (d) $x = 0.22$ and (e) $x = 0.35$. The (h) and (c) indexes refer to the heating and cooling processes, respectively. T_C and T_s refer to the Curie and structural transition temperatures as derived from the magnetometric data, respectively. The structural transition temperature determined from the XRD data is denoted as T_D . The remaining magnetic transition temperatures are marked as T_1 , T_2 and T_t – see the main text for details.

tostructural pressure-temperature (p, T) phase diagrams have been determined (see Figs. 7a–e). Although the magnetic properties are significantly influenced by application of external pressure, some common features are visible in the phase diagrams:

- The temperature of structural martensitic transition T_s is found to decrease almost linearly with increasing hydrostatic pressure for $x = 0.05, 0.1$ and 0.15 . The structural transition is fully ($x = 0.05$; $6 \text{ kbar} \leq p \leq 8 \text{ kbar}$) or partially ($x = 0.1$; ambient pressure) coupled with the transition from para- to

ferromagnetic state for selected chemical compositions and pressure ranges. No structural transition is detected for high Cu content ($x = 0.22$ and 0.35).

- The temperature of transition from para- to magnetically ordered state (T_C for $x = 0.1, 0.15$ and 0.35 ; T_1 for $x = 0.22$) increases linearly with increasing hydrostatic pressure. The $x = 0.05$ case is more complicated, as T_C increases linearly with pressure up to $p = 4$ kbar, then decreases linearly with pressure up to 8 kbar as the magnetic transition is fully coupled with the structural one for intermediate pressures, and finally decreases linearly with lower rate as application of high pressures ($p \geq 10$ kbar) leads to separation of $T_C = 275$ K and T_s which is found below T_C . It is worth noting that for $x = 0.22$, the temperature of a second magnetic transition (T_2) depends on pressure in the same way as T_1 , i.e. both temperatures increase with increasing pressure with the same rate. (see Fig. 7d).
- Additional magnetic transitions, occurring below T_C and marked here as T_t , are observed for $x = 0.1, 0.22$ and 0.35 . For $x = 0.1$, $T_t \approx 180$ K appears only for lower pressures ($p \leq 3$ kbar), where $T_t < T_s$. For $x = 0.22$ and 0.35 , T_t equals around 130 K ($x = 0.22$) or 160 K ($x = 0.35$) at ambient pressure and linearly decreases with applied hydrostatic pressure.

The parameters characterizing pressure-temperature (p, T) phase diagrams of slowly cooled $\text{Co}_{1-x}\text{Cu}_x\text{MnGe}$ ($0.05 \leq x \leq 0.35$) are summarized in Table IV. For comparison, the data for stoichiometric CoMnGe are also included.

III. DISCUSSION

The work reports the results of X-ray diffraction as well as magnetic measurements under applied hydrostatic pressure for $\text{Co}_{1-x}\text{Cu}_x\text{MnGe}$, where x equals 0.05, 0.10, 0.15, 0.22 and 0.35. The X-ray diffraction data collected at low temperature confirm the orthorhombic structure for $x = 0.05, 0.10$ and 0.15 and the hexagonal one for the remaining compounds ($x = 0.22$ and 0.35). With increase of temperature, the orthorhombic martensite structure undergoes a martensitic transformation into the hexagonal austenite one. The transition temperature decreases with increasing Cu content (see Table III). The transition is associated with a distinct jump in the unit cell volume V_o and the lattice parameters a_o and b_o (see Figs. 3a–c). Such a behavior has already been reported for the stoichiometric CoMnGe and is related to the changes in atom positional parameters as well as to the Co thermal parameters being considerably larger in the high-temperature hexagonal structure variant [16]. It is worth noting that the atoms are more densely packed

in the high-temperature hexagonal Ni_2In -type structure when compared with the low-temperature orthorhombic TiNiSi -type one.

The results of magnetic measurements indicate a transition from para- to ferro-/ferrimagnetic state with decreasing temperature (although the transition for $x = 0.22$ involves an intermediate antiferromagnetic phase in limited temperature range). The Curie temperature decreases from 313 K (in the orthorhombic phase) for $x = 0.05$ to about 250 K (in the hexagonal phase) for the remaining compositions ($0.1 \leq x \leq 0.35$).

For all samples the pressure-temperature (p, T) phase diagrams have been determined. For $x = 0.05$, the Curie temperature increases slowly with increasing pressure in the low-pressure range ($p \leq 4$ kbar) – see Fig. 7a. The derivative dT_C/dp equals 1.9(6) K/kbar and is lower than 3.6 K/kbar reported for the stoichiometric CoMnGe [6]. Further increase of pressure leads to appearance of a triple point (p_{TRI}, T_{TRI}) \approx (5 kbar, 325 K), where the structural martensitic transition coincides with para- to ferromagnetic transition. It is worth noting that both p_{TRI} and T_{TRI} take values lower than those found in the stoichiometric CoMnGe ($(p_{TRI}, T_{TRI}) \approx$ (6 kbar, 360 K)) [6]. For pressures $p_{TRI} \leq p \leq 8$ kbar, the para- to ferromagnetic transition remains fully coupled with martensitic transition, which is confirmed by noticeable hysteresis of the susceptibility vs. temperature curves (see Fig. 6a). For the highest pressures ($10 \text{ kbar} \leq p \leq 12 \text{ kbar}$) the second-order para- to ferromagnetic transition (no visible hysteresis) becomes separated from the martensitic transition (well visible hysteresis at lower temperatures). In this pressure range, the Curie temperature decreases with increasing pressure with a rate of -3 K/kbar. The exact values of the dT_C/dp , $dT_s^{(h)}/dp$ and $dT_s^{(c)}/dp$ derivatives, as obtained on heating and cooling, are collected in Table IV. For comparison, the values for $x = 0$ (CoMnGe) are also reported after Ref. [6].

The (p, T) phase diagrams for $x = 0.1$ and 0.15 have common features: the Curie temperature (T_C) increases with increasing pressure with a rate of 1.09(6) K/kbar ($x = 0.1$) or 1.6(2) K/kbar ($x = 0.15$), while the temperature of structural transition (T_s) decreases with increasing pressure with a rate of about -20 K/kbar (the exact values of the transition temperatures and their rates can be found in Table IV. What distinguishes the diagram for $x = 0.1$ is partial magnetostructural coupling of the para- to ferromagnetic transition with the martensitic one at ambient pressure, as well as presence of additional transition ($T_t \approx 180$ K) at low pressures ($0 \leq p \leq 3$ kbar).

The (p, T) phase diagrams for $x = 0.22$ and 0.35 are quite similar one to another as the temperature of transition from para- to magnetically ordered state increases, while T_t decreases with increasing pressure (see Figs. 7d–e). The exact values of the transition temperatures as well as their derivatives over pressure are listed in Table IV.

It is worth noting that the derivatives dT_C/dp in the

TABLE IV. Parameters characterizing pressure-temperature (p, T) phase diagrams of slowly cooled $\text{Co}_{1-x}\text{Cu}_x\text{MnGe}$ ($0 \leq x \leq 0.35$): Curie temperatures (T_C), other magnetic transition temperatures (T_1, T_2, T_t) and temperatures of the structural transition (T_s), together with their derivatives over applied pressure (dT_C/dp , dT_1/dp , dT_2/dp , dT_t/dp , dT_s/dp). The (h) and (c) indices refer to the heating and cooling processes, respectively. γ indicates the Grüneisen parameter derived from the dT_C/dp derivative – see main text for details.

x	T_C [K]	dT_C/dp [K/kbar]	T_t [K]	dT_t/dp [K/kbar]	$dT_s^{(h)}/dp$ [K/kbar]	$dT_s^{(c)}/dp$ [K/kbar]	γ
0*	340	3.6			-11.6	-10.6	8.1
0.05	313	1.9(6)			-12.7(1.3)	-12.7(1.3)	4.5
0.10	250	1.09(6)	180	1.7(2)	-18.5(5)	-21.3(4)	3.2
0.15	260	1.6(2)			-23.1(7)	-21(4)	4.5
0.22	247 (T_1) 235 (T_2)	1.2(2) (dT_1/dp) 1.3(2) (dT_2/dp)	135	-3.4(2)			3.6
0.35	250	1.2(2)	160	-1.3(2)			3.6

* data from Ref. [6].

hexagonal Ni_2In -type structure ($0.1 \leq x \leq 0.35$ – see Figs. 6b–e) equal about 1 K/kbar, which is close to 0.9(1) K/kbar reported for CoMnGe in the metastable Ni_2In -type structure [17].

Magnetostructural phase diagrams reported in this work as well as those of other ternary and pseudoternary $\text{MM}'\text{Ge}$ compounds (where M and M' are transition elements) can be analyzed on the basis of the phenomenological Landau potential [18]:

$$\Phi(\zeta, \eta, p, T) = a[T - T_s(p)]\zeta^2 + e\zeta^4 + k\zeta^6 + b[T - T_C(p)]\eta^2 + f\eta^4 + g\zeta^2\eta^2 \quad (1)$$

where ζ and η refer to the structural and magnetic order parameters, respectively, while a (>0), e (<0), k , b , f (>0) and g (<0) are phenomenological constants. The structural order parameter ζ describes a distortion of the crystal structure, while η is related to magnetization. The terms in Eq. 1 containing solely ζ or η refer to the structural and magnetic transitions, respectively, while the $g\zeta^2\eta^2$ term describes a magnetostructural coupling.

Minimizing the Landau potential given by Eq. 1 with respect to ζ and η leads to the following phases that may appear in the (p, T) phase diagram:

- (i) $\zeta = 0, \eta = 0$ paramagnetic hexagonal phase,
- (ii) $\zeta \neq 0, \eta = 0$ paramagnetic orthorhombic phase,
- (iii) $\zeta = 0, \eta \neq 0$ ferromagnetic hexagonal phase,
- (iv) $\zeta \neq 0, \eta \neq 0$ ferromagnetic orthorhombic phase.

On the (p, T) phase diagram for $x = 0.05$ (see Fig. 7a), the (i), (ii) and (iv) regions are observed. With increasing Cu content the (ii) region vanishes, while the (iii) one develops (see Figs. 7b–c). For the highest Cu contents ($x = 0.22$ and 0.35), only the hexagonal Ni_2In -type crystal structure is observed, and therefore the (i) and

(iii) phases are found in the corresponding phase diagrams (see Figs. 7d–e). The determined (p, T) phase diagrams for the investigated $\text{Co}_{1-x}\text{Cu}_x\text{MnGe}$ compounds for $x = 0.05, 0.10$ and 0.15 (see Figs. 7a–c) are similar to these reported for the isostructural $\text{NiMn}_{1-x}\text{Cr}_x\text{Ge}$ for $x = 0.04, 0.11, 0.18$ and 0.25 (see Figs. 3a–d in Ref. [13]).

On the basis of the experimental data reported in this work, it is possible to calculate the entropy change connected with the martensitic phase transition (both the forward (cooling) and reverse (heating) ones) directly from the Clausius-Clapeyron equation

$$\Delta S = \frac{\Delta v}{\left(\frac{dT_s}{dp}\right)} \quad (2)$$

where Δv is a change of the unit cell volume per unit cell mass at the structural phase transition temperature T_s . For $x = 0.15$, $\Delta v = 5.2 \cdot 10^{-6} \text{ m}^3 \cdot \text{kg}$, according to the data shown in Fig. 3. Taking into account the values of the dT_s/dp derivatives (see Fig. 7c), the entropy change connected with the martensitic phase transition equals 22 and 25 J/(kg · K) for heating and cooling respectively.

Magnetic Grüneisen parameter γ is another quantity that can be calculated on the basis of the experimental data collected in Table IV using the relation

$$\gamma = \frac{d \ln T_C}{d\omega} = \frac{1}{\kappa T_C} \frac{dT_C}{dp} \quad (3)$$

where ω is a relative volume change, while κ is the compressibility (equal in this case $1.36 \cdot 10^{-3} \text{ kbar}^{-1}$ according to Ref. [19]). The Grüneisen parameter can be alternatively defined as $\frac{d \ln J}{d\omega}$, where J is the effective exchange integral. According to the data in Table IV, substituting the Co atoms by the Cu atoms gradually decreases the exchange integral.

In the hexagonal phase the Co atoms have no localized magnetic moments and therefore they do not participate in the magnetic interactions [4]. The magnetic

order is stable solely due to interactions between the Mn magnetic moments. In the orthorhombic phase both the Mn and Co atoms carry magnetic moments [3] and the magnetic order is stable due to interactions between the Mn-Mn, Mn-Co and Co-Co magnetic moments. Higher number of magnetic atoms involved in the magnetic interactions lead to higher Curie temperatures observed in the orthorhombic phase.

The structural and magnetic properties of the investigated $\text{Co}_{1-x}\text{Cu}_x\text{MnGe}$ system are strongly influenced by two types of pressures: the chemical one (resulting from doping the Cu atoms) and the external applied one. Substitution of the Co atoms by the Cu atoms induces positive chemical pressure as confirmed by gradual decrease of the unit cell volume in the orthorhombic crystal phase with increasing Cu content (see Table I and Fig. 3). Both types of pressure have similar influence on the crystal structure and magnetic properties, namely, the increase of pressure stabilizes the hexagonal structure and leads to slow increase of the Curie temperature (except the high pressure range ($p \geq 6$ kbar) for $x = 0.05$, where full magnetostructural coupling is found for $6 \text{ kbar} \leq x \leq 8 \text{ kbar}$ with further separation of the magnetic and structural transitions at higher pressures).

IV. SUMMARY AND CONCLUSIONS

Influence of temperature and applied hydrostatic pressure on structural and magnetic properties of the $\text{Co}_{1-x}\text{Cu}_x\text{MnGe}$ system ($x = 0.05, 0.10, 0.15, 0.22$ and 0.35) is reported. Based on the experimental data the (x, T) and (p, T) magnetostructural phase diagrams have been determined. The presented results indicate that partial substitution of the Co atoms by the Cu atoms strongly influences the physical properties of the investigated compounds, namely:

- a martensitic transition between the low-temperature orthorhombic crystal structure of the TiNiSi -type (space group: $Pnma$) and the high-temperature hexagonal structure of the Ni_2In -type (space group: $P6_3/mmc$) is observed for $x = 0.05, 0.10$ and 0.15 ,
- the martensitic transition from the orthorhombic to the hexagonal structure is accompanied with dis-

tinct decrease of the unit cell volume V and the lattice parameter a as well as an increase of the lattice parameter b ,

- for the high Cu contents ($x = 0.22$ and 0.35) only the hexagonal structure is observed,
- doping the Cu atoms stabilizes the hexagonal crystal structure,
- regardless the crystal structure, the compounds undergo a transition from para- to ferromagnetic state with decreasing temperature (in case of $x = 0.22$ through an intermediate antiferromagnetic phase). The para- to ferromagnetic transition is fully coupled with the martensitic one for $x = 0.05$ at the intermediate pressure range ($6 \text{ kbar} \leq p \leq 8 \text{ kbar}$). Partial magnetostructural coupling is observed for $x = 0.10$ at ambient pressure.
- the Curie temperature at ambient pressure decreases from 313 K for $x = 0.05$ (in the orthorhombic phase) to about 250 K for the remaining compounds (in the hexagonal phase),
- temperature of the structural transition as well as the critical temperature of magnetic ordering decrease with increasing Cu content,
- application of hydrostatic pressure leads to decrease of temperature of the martensitic transition (for $x = 0.05, 0.10$ and 0.15) and slow increase of the critical temperature of magnetic ordering (for all compositions, however, in case of $x = 0.05$ it refers to the low-pressure range ($p \leq 4 \text{ kbar}$) only),
- the determined magnetostructural phase diagrams are explained based on the phenomenological Landau theory.

ACKNOWLEDGEMENTS

We would like to thank Dr. Teresa Jaworska-Gołab from the M. Smoluchowski Institute of Physics, Jagiellonian University, for discussions regarding the XRD measurements.

-
- [1] V. Johnson, Diffusionless orthorhombic to hexagonal transitions in ternary silicides and germanides, *Inorganic Chemistry* 14 (1975) 1117–1120. doi:10.1021/ic50147a032.
- [2] S. Kaprzyk, S. Niziol, The electronic structure of CoMnGe with the hexagonal and orthorhombic crystal structure, *Journal of Magnetism and Magnetic Materials* 87 (1990) 267–275. doi:10.1016/0304-8853(90)90759-J.
- [3] S. Niziol, A. Bombik, W. Bażela, A. Szytuła, D. Fruchart, Crystal and magnetic structure of $\text{Co}_x\text{Ni}_{1-x}\text{MnGe}$ system, *Journal of Magnetism and Magnetic Materials* 27 (1982) 281–292. doi:10.1016/0304-8853(82)90087-7.
- [4] A. Szytuła, A. Pędziwiatr, Z. Tomkiewicz, W. Bażela, Crystal and magnetic structure of CoMnGe , CoFeGe , FeMnGe and NiFeGe , *Journal of Magnetism and Mag-*

- netic Materials 25 (1981) 176–186. doi:10.1016/0304-8853(81)90116-5.
- [5] O. Beckman, L. Lundgren, Chapter 3: Compounds of transition elements with nonmetals, volume 6 of *Handbook of Magnetic Materials*, Elsevier, 1991, pp. 181–287. doi:10.1016/S1567-2719(05)80057-5.
- [6] S. Nizioł, A. Zięba, R. Zach, M. Baj, L. Dmowski, Structural and magnetic phase transitions in $\text{Co}_x\text{Ni}_{1-x}\text{MnGe}$ system under pressure, *Journal of Magnetism and Magnetic Materials* 38 (1983) 205–213. doi:10.1016/0304-8853(83)90046-X.
- [7] J. Zeng, Z. Wang, Z. Nie, Y. Wang, Crystal structural transformation accompanied by magnetic transition in $\text{MnCo}_{1-x}\text{Fe}_x\text{Ge}$ alloys, *Intermetallics* 52 (2014) 101–104. doi:10.1016/j.intermet.2014.03.014, and references therein.
- [8] J. Hamer, R. Daou, S. Özcan, N. Mathur, D. Fray, K. Sandeman, Phase diagram and magnetocaloric effect of $\text{CoMnGe}_{1-x}\text{Sn}_x$ alloys, *Journal of Magnetism and Magnetic Materials* 321 (2009) 3535–3540. doi:10.1016/j.jmmm.2008.03.003, current Perspectives: Magnetocaloric Materials.
- [9] N. T. Trung, V. Biharie, L. Zhang, L. Caron, K. H. J. Buschow, E. Brück, From single- to double-first-order magnetic phase transition in magnetocaloric $\text{Mn}_{1-x}\text{Cr}_x\text{CoGe}$ compounds, *Applied Physics Letters* 96 (2010) 162507. doi:10.1063/1.3399774.
- [10] N. T. Trung, L. Zhang, L. Caron, K. H. J. Buschow, E. Brück, Giant magnetocaloric effects by tailoring the phase transitions, *Applied Physics Letters* 96 (2010) 172504. doi:10.1063/1.3399773.
- [11] H. Zhang, Y. Li, E. Liu, K. Tao, M. Wu, Y. Wang, H. Zhou, Y. Xue, C. Cheng, T. Yan, K. Long, Y. Long, Multiple magnetic transitions in $\text{MnCo}_{1-x}\text{Cu}_x\text{Ge}$ driven by changes in atom separation and exchange interaction, *Materials & Design* 114 (2017) 531–536. doi:10.1016/j.matdes.2016.10.066.
- [12] S. Pal, C. Frommen, S. Kumar, B. Hauback, H. Fjellvåg, T. Woodcock, K. Nielsch, G. Helgesen, Comparative phase transformation and magnetocaloric effect study of Co and Mn substitution by Cu in MnCoGe compounds, *Journal of Alloys and Compounds* 775 (2019) 22–29. doi:10.1016/j.jallcom.2018.10.040.
- [13] R. Duraj, A. Szytuła, T. Jaworska-Gołąb, A. Deptuch, Y. Tyvanchuk, A. Sivachenko, V. Val'kov, V. Dyakonov, Pressure effect on magnetic phase transitions in slowly cooled $\text{NiMn}_{1-x}\text{Cr}_x\text{Ge}$, *Journal of Alloys and Compounds* 741 (2018) 449–453. doi:10.1016/j.jallcom.2018.01.064.
- [14] A. Deptuch, R. Duraj, A. Szytuła, B. Penc, E. Juszyńska-Gałązka, S. Baran, Tuning magnetostructural phase transition in $\text{CoMn}_{0.88}\text{Cu}_{0.12}\text{Ge}$ by application of hydrostatic pressure, *Scripta Materialia* 218 (2022) 114823. doi:10.1016/j.scriptamat.2022.114823.
- [15] J. Rodríguez-Carvajal, Recent advances in magnetic structure determination by neutron powder diffraction, *Physica B: Condensed Matter* 192 (1993) 55–69. doi:10.1016/0921-4526(93)90108-I.
- [16] W. Jeitschko, A high-temperature X-ray study of the displacive phase transition in MnCoGe , *Acta Crystallographica Section B* 31 (1975) 1187–1190. doi:10.1107/S0567740875004773.
- [17] R. Zach, R. Duraj, A. Szytuła, Pressure effect on magnetic transformations in the $\text{Co}_x\text{Ni}_{1-x}\text{MnGe}$ system, *physica status solidi (a)* 84 (1984) 229–236. doi:10.1002/pssa.2210840129.
- [18] L. D. Landau, E. M. Lifshitz, *Statistical physics*, volume 5 of *Course of Theoretical Physics*, Pergamon Press, 1969. 2nd edition.
- [19] R. Zach, PhD thesis, Jagiellonian University, Kraków, Poland, 1984.